# Renormalization of Transverse-Momentum-Dependent Parton Distribution on the Lattice

Kuan Zhang,[1,2] Xiangdong Ji,[3] Yi-Bo Yang,[1,2,4,5,*] Fei Yao,[6] and Jian-Hui Zhang[6,†]

[Lattice Parton Collaboration (LPC)]

[1]*University of Chinese Academy of Sciences, School of Physical Sciences, Beijing 100049, China*
[2]*CAS Key Laboratory of Theoretical Physics, Institute of Theoretical Physics, Chinese Academy of Sciences, Beijing 100190, China*
[3]*Department of Physics, University of Maryland, College Park, Maryland 20742, USA*
[4]*School of Fundamental Physics and Mathematical Sciences, Hangzhou Institute for Advanced Study, UCAS, Hangzhou 310024, China*
[5]*International Centre for Theoretical Physics Asia-Pacific, Beijing/Hangzhou, China*
[6]*Center of Advanced Quantum Studies, Department of Physics, Beijing Normal University, Beijing 100875, China*

(Received 2 June 2022; accepted 29 July 2022; published 16 August 2022)

To calculate the transverse-momentum-dependent parton distribution functions (TMDPDFs) from lattice QCD, an important goal yet to be realized, it is crucial to establish a viable nonperturbative renormalization approach for linear divergences in the corresponding Euclidean quasi-TMDPDF correlators in large-momentum effective theory. We perform a first systematic study of the renormalization property of the quasi-TMDPDFs by calculating the relevant matrix elements in a pion state at five lattice spacings ranging from 0.03 fm to 0.12 fm. We demonstrate that the square root of the Wilson loop combined with the short distance hadron matrix element provides a successful method to remove all ultraviolet divergences of the quasi-TMD operator, and thus provides the necessary justification to perform a continuum limit calculation of TMDPDFs. In contrast, the popular regularization independent momentum subtraction renormalization (RI/MOM) scheme fails to eliminate all linear divergences.

DOI: 10.1103/PhysRevLett.129.082002

*Introduction.*—Parton distribution functions (PDFs) offer an effective description of quarks and gluons inside a light-traveling hadron [1,2], and play an essential role in understanding many processes in high-energy and hadron physics. As a natural generalization of the collinear PDFs, the transverse-momentum-dependent (TMD) PDFs also encompass the transverse momentum of partons, and thus provide a useful description of the transverse structure of hadrons. They are also crucial inputs for describing multiscale, noninclusive observables at high-energy colliders such as the LHC [3]. Understanding the transverse-momentum-dependent parton distribution functions (TMDPDFs) has been an important goal of many experimental facilities around the world, such as COMPASS at CERN, JLab 12 GeV upgrade, RHIC, and in particular, the forthcoming Electron-Ion Collider in the U.S. Currently, our knowledge of TMDPDFs mainly comes from studies of Drell-Yan and semi-inclusive deep-inelastic scattering processes where the transverse momenta of final state particles are measured. In the past, various fittings have been carried out to extract the TMDPDFs from these data (see, e.g., Refs. [4–9]). However, calculating the TMDPDFs from first principles has been a challenge, as they are nonperturbative quantities defined in terms of light-cone correlations.

Thanks to the theoretical developments, especially of large-momentum effective theory (LMET) [10,11], in the past few years, such calculations have become feasible, but full TMDPDFs from a lattice are not yet available. Instead of the standard TMDPDFs involving light-cone Wilson links, LMET proposes to calculate the quasi-TMDPDF defined by a quark bilinear operator with a staple-shaped Wilson link of finite length along the spacelike direction. The finite link length regulates the so-called pinch-pole singularity associated with infinitely long Wilson lines [11]. The singular dependence on such a link length is then canceled by the square root of a Euclidean Wilson loop which, in the mean time, also cancels most of the ultraviolet (uv) divergences (except for the endpoint logarithmic uv divergences which need to be canceled by other means). The renormalized quasi-TMDPDF can then be factorized into the standard TMDPDF associated with a perturbative hard kernel, a Collins-Soper evolution part and an "intrinsic soft function," up to power suppressed contributions [11–13].

Although there have been some preliminary lattice studies of the Collins-Soper evolution kernel and the intrinsic soft function [14–19], an important piece of information is still missing in realizing the lattice calculation of TMDPDFs, that is, a systematic study of the nonperturbative renormalization of quasi-TMDPDF operators. This is highly nontrivial, given that both the regularization independent momentum subtraction (RI MOM) [20] and the Wilson line or loop renormalization fail to cancel the power uv divergences in the case of straight-line quasi-PDF operators [21]. It is the purpose of this Letter to perform such a systematic analysis and to find a viable nonperturbative renormalization approach for the quasi-TMDPDFs, such as the hybrid scheme [22] with self-renormalization in the case of quasi-PDFs [23]. Indeed, our study shows that the square root of the Wilson loop combined with short-distance hadron matrix elements is able to eliminate all uv divergences of the quasi-TMDPDF operator and thus ensures a well-defined continuum limit, while the RI/MOM scheme fails in a way similar to that in the quasi-PDF case.

*Theoretical framework.*—In LMET, the calculation of TMDPDFs starts from the unsubtracted quasi-TMDPDF defined as

$$\tilde{h}_{\chi,\gamma_t}(b,z,L,P_z;1/a) = \langle\chi(P_z)|O_{\gamma_t}(b,z,L)|\chi(P_z)\rangle,$$
$$O_\Gamma(b,z,L) \equiv \bar{\psi}(\vec{0}_\perp,0)\Gamma\mathcal{W}(b,z,L)\psi(\vec{b}_\perp,z), \quad (1)$$

where we have taken the unpolarized case with $\Gamma=\gamma^t$ as an illustrative example, and assumed a lattice regularization with spacing $a$. $\chi(P_z)$ denotes the hadron state with momentum $P_\mu=(P_0,0,0,P_z)$, and the quark bilinear operator $O_\Gamma(b,z,L)$ contains a staple-shaped Wilson link $\mathcal{W}(b,z,L)$ shown in Fig. 1 and defined as

$$\begin{aligned}\mathcal{W}(b,z,L) = &\mathcal{P}\exp\left[ig_s\int_{-L}^{z} ds\,\hat{n}_z\cdot A(b\hat{n}_\perp+s\hat{n}_z)\right]\\ &\times\mathcal{P}\exp\left[ig_s\int_{0}^{b} ds\,\hat{n}_\perp\cdot A(s\hat{n}_\perp-L\hat{n}_z)\right]\\ &\times\mathcal{P}\exp\left[ig_s\int_{0}^{-L} ds\,\hat{n}_z\cdot A(s\hat{n}_z)\right], \end{aligned}\quad (2)$$

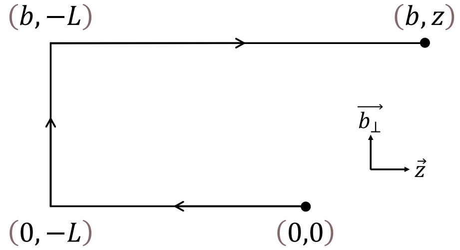


FIG. 1. Illustration of the structure of the Wilson line $\mathcal{W}(b,z,L)$ needed by the quasi-TMDPDF operator.

where $b=|\vec{b}_\perp|$ and $z$ are the separation between the two quark fields along the transverse direction $\hat{n}_\perp$ and longitudinal direction $\hat{n}_z$, respectively. $L$ should be large enough to approximate the infinitely long Wilson link in the continuum.

Such a definition suffers from the pinch-pole singularity as well as the linear divergence from the Wilson link self-energy, both of which are associated with the length $L$. A more convenient "subtracted" quasi-TMDPDF is then formed as [12]

$$h_{\chi,\gamma_t}(b,z,P_z;1/a) = \lim_{L\to\infty}\frac{\tilde{h}_{\chi,\gamma_t}(b,z,L,P_z;1/a)}{\sqrt{Z_E(b,2L+z;1/a)}}, \quad (3)$$

where we have assumed a lattice regularization and included $1/a$ dependence in the matrix elements. $Z_E(b,2L+z)$ is the rectangle Wilson loop with side lengths $b$ and $2L+z$. In $h_{\chi,\gamma_t}(b,z,P_z;1/a)$, the pinch-pole singularity, the linear divergences, as well as the cusp divergences are canceled, but there still remain logarithmic divergences arising from the endpoint of the Wilson links which require further renormalization.

Since the uv divergence is of a multiplicative structure [24,25] and independent of the external state, the remaining logarithmic divergences of the subtracted quasi-TMDPDF can be removed either by dividing by another subtracted quasi-TMDPDF at zero momentum and short distances $b_0$ and $z_0$, in analogy with the ratio scheme in the quasi-PDF case [26], or by dividing by an appropriate ratio formed by the quasi-PDF matrix elements at zero momentum and short distances [27]. Here we choose the first option as an illustrative example. In the above renormalization, we work with physical on shell matrix elements only, and therefore do not suffer from operator mixings due to off shellness in the RI/MOM scheme. Nevertheless, for nonchiral lattice fermion actions there could be mixings between the quasi-TMDPDF operator with $\Gamma=\gamma^t$ and $\Gamma=\gamma^t\gamma^3$ due to chiral symmetry breaking [27]. However, their numerical impact appears to be negligibly small [14]. Therefore, for the purpose of demonstrating the cancellation of uv divergences, we ignore it here.

We write the fully renormalized quasi-TMDPDF as

$$h^{\rm SDR}_{\chi,\gamma_t}\left(b,z,P_z;\frac{1}{b_0}\right) = \frac{h_{\chi,\gamma_t}(b,z,P_z;1/a)}{h_{\pi,\gamma_t}(b_0,z_0=0,0,1/a)}, \quad (4)$$

where we have used a superscript SDR to denote the short-distance ratio (SDR) scheme, and chosen the pion matrix element in the denominator (denoted by the subscript $\pi$). For simplicity, we have also chosen $z_0=0$. The singular dependence on $a$ on the rhs of Eq. (4) has been canceled, leaving a dependence on the perturbative short scale $b_0$. To perform the renormalization, the pion matrix element

$h_{\pi,\gamma_t}(b_0,0,0,1/a)$ needs to be calculated nonperturbatively on the lattice. In order to match the renormalized quasi-TMDPDF to the standard TMDPDF, we also need the perturbative results of the above matrix elements, for which we can choose on shell quark external states. The numerator of the rhs of Eq. (4) has been calculated previously in dimensional regularization (DR) and modified minimal subtraction ($\overline{\mathrm{MS}}$) scheme in Ref. [13], whereas the denominator is independent of $\chi$ and reads as [28]

$$h^{\overline{\mathrm{MS}}}_{\chi,\gamma_t}(b_0,z_0,0;\mu)=1+\frac{\alpha_s C_F}{2\pi}\left\{\frac{1}{2}+3\gamma_E-3\ln 2+\frac{3}{2}\ln[\mu^2(b_0^2+z_0^2)]-2\frac{z_0}{b_0}\arctan\frac{z_0}{b_0}\right\}+\mathcal{O}(\alpha_s^2). \tag{5}$$

With this, we can also convert the SDR result to the $\overline{\mathrm{MS}}$ scheme via

$$h^{\overline{\mathrm{MS}}}_{\chi,\gamma_t}(b,z,P_z;\mu)=h^{\overline{\mathrm{MS}}}_{\gamma_t}(b_0,0,0;\mu)h^{\mathrm{SDR}}_{\chi,\gamma_t}\left(b,z,P_z;\frac{1}{b_0}\right), \tag{6}$$

where $b_0$ dependence cancels.

Another renormalization option that has been studied in the literature is the RI/MOM renormalization [20] with the perturbative matching to the $\overline{\mathrm{MS}}$ scheme [13,29],

$$\begin{aligned}h^{\mathrm{MOM}}_{\chi,\Gamma}(b,z,P_z;p)&=\sum_{\Gamma'}[Z^{\mathrm{MOM}}(b,z,p;1/a)]^{-1}_{\Gamma\Gamma'}h_{\chi,\Gamma'}(b,z,P_z;1/a)\\&=\lim_{L\to\infty}\sum_{\Gamma'}\tilde{Z}^{\mathrm{MOM}}(b,z,L,p;1/a)]^{-1}_{\Gamma\Gamma'}\tilde{h}_{\chi,\Gamma'}(b,z,L,P_z;1/a),\end{aligned} \tag{7}$$

$$h^{\overline{\mathrm{MS}}}_{\chi,\gamma_t}(b,z,P_z;\mu)=\sum_{\Gamma}\mathrm{Tr}[\Gamma h_{q(p),\gamma_t}(b,z,p_z)]^{\overline{\mathrm{MS}}}(\mu)h^{\mathrm{MOM}}_{\chi,\Gamma}(b,z,P_z;p), \tag{8}$$

where $[\tilde{Z}^{\mathrm{MOM}}]_{\Gamma\Gamma'}=\mathrm{Tr}[\Gamma'\tilde{h}_{q(p),\Gamma}]$ is the matrix element of $\mathcal{O}_\Gamma$ in the off shell quark state $q$ with momentum $p$ and projector $\Gamma'$. The $\sqrt{Z_E}$ factor gets canceled between the nonperturbative renormalization factor $[Z^{\mathrm{MOM}}]_{\Gamma\Gamma'}=\mathrm{Tr}[\Gamma' h_{q(p),\Gamma'}]$ and the bare hadron matrix element $h_\chi$, but this does not affect the cancellation of singular $L$ dependence between them; thus one can safely take the large-$L$ limit. In Eq. (8) the dependence on the four-momentum $p$ on the rhs gets canceled between the two terms up to discretization errors.

The off diagonal components of $Z^{\mathrm{MOM}}$ can be sizable [30] in general, but they turn out to be suppressed with the momentum setup $p_z=p_\perp=0$ [14]. When the off diagonal components of $Z^{\mathrm{MOM}}$ are negligible, Eq. (7) can be simplified into

$$h^{\overline{\mathrm{MS}},\mathrm{MOM}}_{\chi,\gamma_t}(b,z,P_z;\mu)\simeq\frac{\mathrm{Tr}[\gamma_t h_{q(p),\gamma_t}(b,z,p_z)]^{\overline{\mathrm{MS}}}(\mu)}{\mathrm{Tr}[\gamma_t h_{q(p),\gamma_t}(b,z,p_z;1/a)]}\times h_{\chi,\gamma_t}(b,z,P_z;1/a). \tag{9}$$

*Simulation setup.*—In this Letter, we use the clover valence quark on the $2+1+1$ flavors (degenerate up and down, strange, and charm degrees of freedom) of highly improved staggered quarks and one-loop Symanzik improved [31] gauge ensembles from the MILC Collaboration [32–34] at five lattice spacings. We tuned the valence light quark mass to be around that in the sea, and the information about the ensembles and parameters we used are listed in Table I.

Since the uv divergence shall be independent of the hadron state, as shown in the quasi-PDF case [21,23], in the following we will concentrate on the pion matrix element $\tilde{h}_\pi(b,z,L)\equiv\langle\pi|O_{\gamma_t}(b,z,L)|\pi\rangle$ of the quasi-TMDPDF operator $O_{\gamma_t}(b,z,L)$ as an illustrative example, which can be extracted from the following ratio

$$\begin{aligned}R_\pi(t_1,b,z,L;a,t_2)&\equiv\frac{\langle O_\pi(t_2)\sum_{\vec{x}}O_\Gamma[b,z,L;(\vec{x},t_1)]O^\dagger_\pi(0)\rangle}{\langle O_\pi(t_2)O^\dagger_\pi(0)\rangle}\\&=\langle\pi|O_\Gamma(b,z,L)|\pi\rangle+\mathcal{O}(e^{-\Delta m t_1},e^{-\Delta m(t_2-t_1)},e^{-\Delta m t_2}),\end{aligned} \tag{10}$$

where $\Delta m$ is the mass gap between the pion and its first excited state which is around 1 GeV. One-step hypercubic (HYP) smearing is applied on the staple-shaped link to enhance the signal to noise ratio (SNR), and our previous studies [21,23] on the quasi-PDF operator suggest that such a smearing will not change the renormalization behavior of the results. The source or sink setup and also the ground state matrix element extraction are similar to those in Refs. [21,23].

The square root of the Wilson loop $Z_E(b,2L+z)$ is expected to cancel the linear divergence in $h_\pi$, but its SNR

TABLE I. Setup of the ensembles, including the bare coupling constant $g$, lattice size $L^3\times T$, and lattice spacing $a$. $m_q^w$ is the bare quark masses. The pion masses in the sea are ~310 MeV, and the valence pion mass is in the range of 280–320 MeV.

| Tag | $6/g^2$ | $L$ | $T$ | $a$ (fm) | $m_q^{\mathrm{w}}a$ | $c_{\mathrm{sw}}$ |
|---|---|---|---|---|---|---|
| MILC12 | 3.60 | 24 | 64 | 0.1213(9) | −0.0695 | 1.0509 |
| MILC09 | 3.78 | 32 | 96 | 0.0882(7) | −0.0514 | 1.0424 |
| MILC06 | 4.03 | 48 | 144 | 0.0574(5) | −0.0398 | 1.0349 |
| MILC04 | 4.20 | 64 | 192 | 0.0425(5) | −0.0365 | 1.0314 |
| MILC03 | 4.37 | 96 | 288 | 0.0318(5) | −0.0333 | 1.0287 |

can be very poor at large $b$ and/or $2L+z$. The estimate of $Z_E(b,2L+z)$ with finite statistics can even lead to a negative central value and make $\sqrt{Z_E(b,2L+z)}$ ill defined. But since $Z_E(b,2L+z)\underset{L\to\infty}{\to} C(b)e^{-V(b)(2L+z)}$ where $V(b)$ is the QCD static potential, we can fit $Z_E(b,2L+z)$ by a single exponential term at large $L$ and replace it with the fit result. Such a replacement is essential to access the large $b$ and $z$ region at small lattice spacing.

For the RI/MOM renormalization, we choose the to-and-fro and transverse gauge links to be along the $z$ and $x$ directions, respectively, and set the external momentum to be $(p_x,p_y,p_z,p_t)=(2\pi/L)(0,5,0,5)$ on all five ensembles. Such a setup avoids the momentum along the link direction, and thus there is no imaginary part in the quark matrix element projected with $\gamma_t$. $|p|\simeq 3$ GeV is, on the one hand, large enough to suppress the ir effect, and on the one hand, not too huge to yield obvious discretization errors at the largest lattice spacing.

The details of the Wilson loop extrapolation and $L$ dependence of $h_{\pi,\gamma_t}$ and $h^{\mathrm{MOM}}_{\pi,\gamma_t}$ can also be found in the Supplemental Material [28].

*Numerical results.*—With a constant fit in the range $L\geq 0.36$ fm, one can extract the RI MOM renormalized matrix element $h^{\mathrm{MOM}}_{\pi,\gamma_t}(b,z,0;\mu_{\mathrm{MOM}}\simeq 3\text{ GeV})$. Thanks to the cancellation between the $L$ dependence of $\tilde{h}_\pi$ and $\tilde{Z}^{\mathrm{MOM}}$, the $L$ needed to reach saturation is much smaller than that needed for $h_\pi$ defined in Eq. (3). We interpolate the results to $b=0.12$ fm with the cubic spline algorithm, and plot the results at different lattice spacings in Fig. 2. It is clear that the lattice spacing dependence becomes stronger with either larger $z$ or smaller $a$, implying that there are residual linear divergences in $h^{\mathrm{MOM}}_{\pi,\gamma_t}$. In other words, the RI MOM renormalization does not cancel all the linear divergences. As suggested by the quasi-PDF study [21], the residual linear divergence in $h^{\mathrm{MOM}}_{\pi,\gamma_t}$ does not appear at the one-loop level, and shall be gauge- and action-dependent occurring at higher orders. Since the matching between the RI MOM and $\overline{\mathrm{MS}}$ scheme is calculated under DR in which the linear divergence is absent, we expect $h^{\overline{\mathrm{MS}},\mathrm{MOM}}_{\pi,\gamma_t}$ to inherit the residual linear divergence issue and do not consider it any more in the discussion to follow.

We also repeat the above calculations with the overlap fermion action, and find that the pion matrix elements are independent of the fermion action within statistical uncertainties, while the quark matrix elements needed by the RI MOM renormalization can be very sensitive to the fermion action. It is similar to what we observed for the quasi-PDF with a straight Wilson link [21]. Thus, in the main text above we only concentrate on the clover fermion action, and leave the comparison between different fermion actions to the Supplemental Material [28]. The discussion on the lattice spacing dependence of the off diagonal components of $Z^{\mathrm{MOM}}$ can also be found there.

Now we consider the SDR scheme. As mentioned earlier, the subtracted quasi-TMDPDF matrix element contains logarithmic uv divergences, which shall be canceled by the short $b$ and $z$ matrix elements at zero momentum. This is illustrated in Fig. 3 for the choice $z=0$, where we have converted the SDR result to the $\overline{\mathrm{MS}}$ scheme using Eq. (6). As shown in the figure, the results at different lattice spacings exhibit a convergence behavior within errors. Moreover, there is an agreement with the perturbative $\overline{\mathrm{MS}}$ one-loop result (dense dashed line) in the range of $b<0.4$ fm with the $\overline{\mathrm{MS}}$ scale 2 GeV. We also

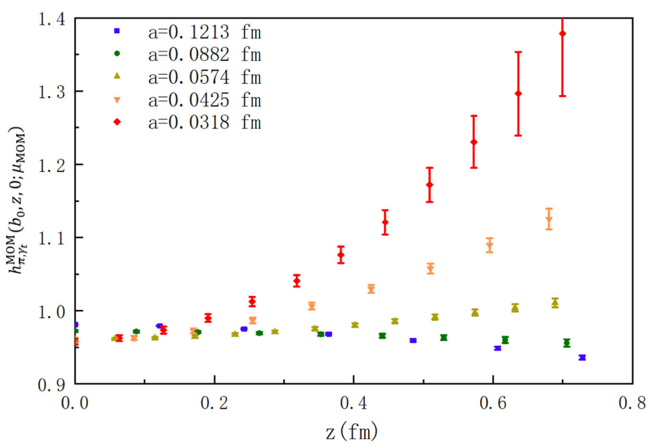


FIG. 2. The RI/MOM renormalized matrix elements $h^{\mathrm{MOM}}_{\pi,\gamma_t}(b_0,z,0;\mu_{\mathrm{MOM}})$ defined in Eq. (7) using the clover fermion action, with $b_0=0.12$ fm and $\mu_{\mathrm{MOM}}\simeq 3$ GeV. The statistical uncertainty comes from bootstrap resampling. We use the cubic spline algorithm to interpolate $b$ to the same value for different lattice spacings.

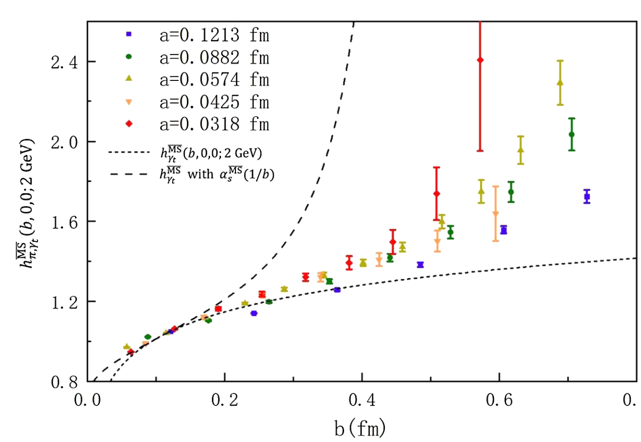


FIG. 3. The renormalized matrix elements $h^{\overline{\mathrm{MS}}}_{\pi,\gamma_t}(b,0,0;2\text{ GeV})$ defined in Eq. (6) and the statistical uncertainty come from bootstrap resampling. The dense dashed line is the one-loop result with $\alpha_s(2\text{ GeV})$ in the $\overline{\mathrm{MS}}$ scheme. We also show a sparse dashed line for the perturbative result with $\alpha_s(1/b)$ for comparison.

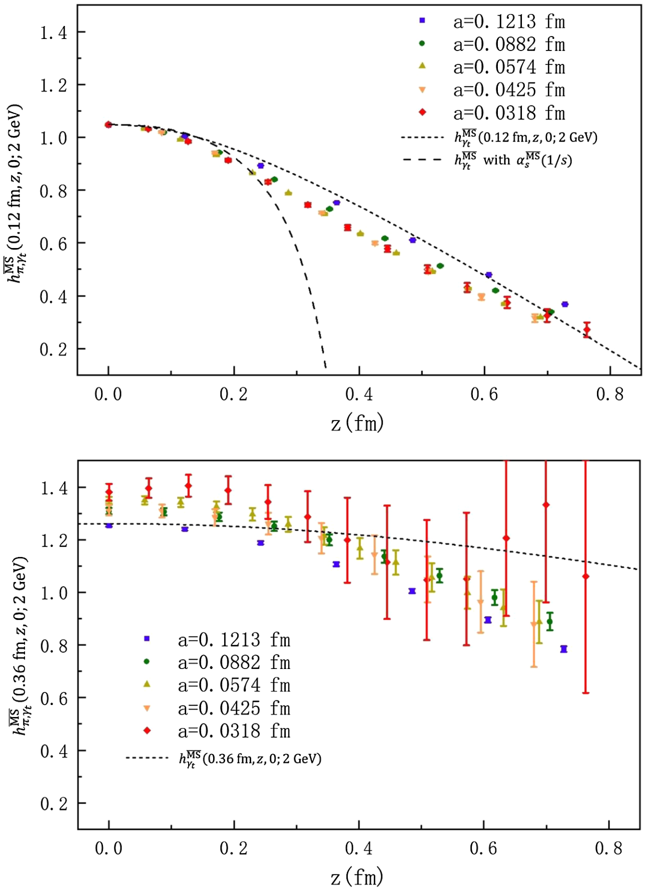


FIG. 4. The renormalized matrix elements $h^{\overline{\rm MS}}_{\pi,\gamma_t}(b, z, 0; 2\ \text{GeV})$ defined in Eq. (6). The black line is the result in the one-loop level. The upper figure is calculated with $b = 0.12$ fm, and the lower figure is calculated with $b = 0.36$ fm. Note that $b$ has been interpolated to the same value but $z$ are kept original. The statistical uncertainty comes from bootstrap resampling. The dense dashed line is the one-loop result with $\alpha_s(2\ \text{GeV})$ in the $\overline{\rm MS}$ scheme. We also show a sparse dashed line for the perturbative result with $\alpha_s(1/s)$, $s = \sqrt{b^2 + z^2}$ for comparison.

show sparse dashed lines for the one-loop results with $\alpha_s(1/b)$ for comparison.

In Fig. 4, we show the renormalized $h^{\overline{\rm MS}}_{\pi,\gamma_t}$ at $b = 0.12$ fm and 0.36 fm as a function of $z$. The same figures for other values of $b$ up to 0.72 fm, and for the case of the TMD wave function matrix element can be found in the Supplemental Material [28]. In contrast with the $h^{\rm MOM}_{\pi,\gamma_t}$ shown in Fig. 2, the $h^{\overline{\rm MS}}_{\pi,\gamma_t}$ shows good convergence in the continuum limit, regardless of the value of $z$ and $b$, and agrees with the perturbative value well when $b$ is small. Thus the renormalized TMD-PDF matrix element using the SDR scheme can actually eliminate all the uv divergence and be insensitive to the subtraction point $b_0$ (or $z_0$), and then can be used for a state-of-the-art TMDPDF calculation on the lattice.

*Summary and outlook.*—In this Letter, we study systematically the renormalization property of the quasi-TMDPDFs. By calculating the pion matrix elements in the rest frame at five lattice spacings and applying different renormalizations, we find that the RI/MOM renormalized matrix element has an obvious residual linear divergence. In contrast, the square root of the rectangular Wilson loop can eliminate all the linear divergence in the hadron matrix element of the quasi-TMDPDF operator, and the remaining logarithmic divergence can be removed by forming the ratio with a subtracted quasi-TMDPDF matrix element at zero momentum and short $b$ and $z$, thus leading to a well-defined continuum limit.

In summary, this Letter provides a crucial test and establishes a viable solution for the renormalization of the quasi-TMD hadron matrix element on the lattice, ensuring the existence of a reliable continuum extrapolation. It paves the way toward the nonperturbative prediction of both TMDPDF and TMD wave functions on the lattice.

We thank the MILC collaboration for providing us with their gauge configurations, $\chi$QCD collaboration for sharing the overlap fermion propagators on those ensembles, and Andreas Schäfer, Wei Wang, and Yu-Shan Su for useful information and discussions. The calculations were performed using the CHROMA software suite [35] with QUDA [36–38] through HIP programming model [39]. The numerical simulations were carried out on the SunRising-1 computing platform, and supported by Strategic Priority Research Program of Chinese Academy of Sciences, Grant No. XDC01040100, and HPC Cluster of ITP-CAS. Y. Yang is supported by the Strategic Priority Research Program of Chinese Academy of Sciences, Grants No. XDB34030303 and No. XDPB15, and also Project 12047503 supported by NSFC. Y. Yang and J.-H. Zhang are also supported by a NSFC-DFG joint grant under Grant No. 12061131006 and SCHA 458/22.

*Corresponding author.
ybyang@itp.ac.cn
†Corresponding author.
zhangjianhui@bnu.edu.cn

[1] R. Ellis, W. Stirling, and B. Webber, *QCD and Collider Physics*, (Cambridge University Press, Cambridge, England, 2011), Vol. 8.
[2] A. W. Thomas and W. Weise, *The Structure of the Nucleon* (Wiley, Germany, 2001).
[3] M. Constantinou *et al.*, Prog. Part. Nucl. Phys. **121**, 103908 (2021).
[4] A. Bacchetta, F. Delcarro, C. Pisano, M. Radici, and A. Signori, J. High Energy Phys. 06 (2017) 081; 06 (2019) 051(E).
[5] I. Scimemi and A. Vladimirov, Eur. Phys. J. C **78**, 89 (2018).
[6] V. Bertone, I. Scimemi, and A. Vladimirov, J. High Energy Phys. 06 (2019) 028.
[7] I. Scimemi and A. Vladimirov, J. High Energy Phys. 06 (2020) 137.

[8] A. Bacchetta, V. Bertone, C. Bissolotti, G. Bozzi, F. Delcarro, F. Piacenza, and M. Radici, J. High Energy Phys. 07 (2020) 117.

[9] A. Bacchetta, F. Delcarro, C. Pisano, and M. Radici, Phys. Lett. B **827**, 136961 (2022).

[10] X. Ji, Phys. Rev. Lett. **110**, 262002 (2013).

[11] X. Ji, Y. Liu, Y. S. Liu, J.-H. Zhang, and Y. Zhao, Rev. Mod. Phys. **93**, 035005 (2021).

[12] X. Ji, Y. Liu, and Y.-S. Liu, Nucl. Phys. **B955**, 115054 (2020).

[13] M. A. Ebert, I. W. Stewart, and Y. Zhao, J. High Energy Phys. 09 (2019) 037.

[14] Q.-A. Zhang, J. Hua, Y. Huo, X. Ji, Y. Liu, Y.-S. Liu, M. Schlemmer, A. Schäfer, P. Sun, W. Wang, and Y.-B. Yang (Lattice Parton Collaboration), Phys. Rev. Lett. **125**, 192001 (2020).

[15] Y. Li *et al.*, Phys. Rev. Lett. **128**, 062002 (2022).

[16] M.-H. Chu *et al.* (LPC Collaboration), arXiv:2204.00200 [Phys. Rev. D (to be published)].

[17] P. Shanahan, M. Wagman, and Y. Zhao, Phys. Rev. D **102**, 014511 (2020).

[18] P. Shanahan, M. Wagman, and Y. Zhao, Phys. Rev. D **104**, 114502 (2021).

[19] M. Schlemmer, A. Vladimirov, C. Zimmermann, M. Engelhardt, and A. Schäfer, J. High Energy Phys. 08 (2021) 004.

[20] G. Martinelli, C. Pittori, C. T. Sachrajda, M. Testa, and A. Vladikas, Nucl. Phys. **B445**, 81 (1995).

[21] K. Zhang, Y.-Y. Li, Y.-K. Huo, A. Schäfer, P. Sun, and Y.-B. Yang ($\chi$QCD Collaboration), Phys. Rev. D **104**, 074501 (2021).

[22] X. Ji, Y. Liu, A. Schfer, W. Wang, Y.-B. Yang, J.-H. Zhang, and Y. Zhao, Nucl. Phys. **B964**, 115311 (2021).

[23] Y.-K. Huo *et al.* (Lattice Parton Collaboration), Nucl. Phys. **B969**, 115443 (2021).

[24] M. A. Ebert, I. W. Stewart, and Y. Zhao, J. High Energy Phys. 03 (2020) 099.

[25] J. R. Green, K. Jansen, and F. Steffens, Phys. Rev. D **101**, 074509 (2020).

[26] A. V. Radyushkin, Phys. Rev. D **96**, 034025 (2017).

[27] Y. Ji, J.-H. Zhang, S. Zhao, and R. Zhu, Phys. Rev. D **104**, 094510 (2021).

[28] See Supplemental Material at http://link.aps.org/supplemental/10.1103/PhysRevLett.129.082002 for the 1-loop calculation of the quasi-TMD matrix element, Wilson loop extrapolation and L dependence, action dependence and operator mixing, and also the renormalized matrix element of the quasi-TMDPDF and quasi-TMDWF matrix elements.

[29] M. Constantinou, H. Panagopoulos, and G. Spanoudes, Phys. Rev. D **99**, 074508 (2019).

[30] P. Shanahan, M. L. Wagman, and Y. Zhao, Phys. Rev. D **101**, 074505 (2020).

[31] A. Hart, G. M. von Hippel, and R. R. Horgan (HPQCD Collaboration), Phys. Rev. D **79**, 074008 (2009).

[32] A. Bazavov *et al.* (MILC Collaboration), Phys. Rev. D **82**, 074501 (2010).

[33] A. Bazavov *et al.* (MILC Collaboration), Phys. Rev. D **87**, 054505 (2013).

[34] A. Bazavov, C. Bernard, N. Brown, C. DeTar, A. X. El-Khadra *et al.*, Phys. Rev. D **98**, 074512 (2018).

[35] R. G. Edwards and B. Joo (SciDAC, LHPC, UKQCD Collaborations), Nucl. Phys. B, Proc. Suppl. **140**, 832 (2005).

[36] M. A. Clark, R. Babich, K. Barros, R. C. Brower, and C. Rebbi, Comput. Phys. Commun. **181**, 1517 (2010).

[37] R. Babich, M. A. Clark, B. Joo, G. Shi, R. C. Brower, and S. Gottlieb, in *SC11 International Conference for High Performance Computing, Networking, Storage and Analysis, Seattle, Washington, 2011* (Association for Computing Machinery, New York, 2011), arXiv:1109.2935.

[38] M. A. Clark, B. Jo, A. Strelchenko, M. Cheng, A. Gambhir, and R. Brower, arXiv:1612.07873.

[39] Y.-J. Bi, Y. Xiao, M. Gong, W.-Y. Guo, P. Sun, S. Xu, and Y.-B. Yang, *Proc. Sci.*, LATTICE2019 (2020) 286 [arXiv:2001.05706].